Transactions on Energy Systems and Engineering Applications

*Article*

# Integration of state of health in power management algorithms for hybrid renewable energy systems

**Siddharth Joshi[1,2,*], Akash V. Barva[3,4] and Digesh D. Shah[5]**

1 Assistant Professor, Department of Electrical Engineering, School of Energy Technology, Pandit Deendayal Energy University, Gandhinagar 382426, Gujarat, India.
2 Non-executive Consultant, APA Groups, 9 Lymington Road, Stafford ST16 3SQ, United Kingdom.
3 Research Scholar, Department of Electrical Engineering, School of Energy Technology, Pandit Deendayal Energy University, Gandhinagar 382426, Gujarat, India.
4 Assistant Manager, Research and Development, Atul Greentech Private Limited, Ahmedabad 382240, Gujarat, India.
5 Assistant Professor, Parul Institute of Engineering and Technology, Parul University, Vadodara 391760, Gujarat, India.
* Correspondence: siddharth.joshi@sot.pdpu.ac.in

*Received: 15 March 2025; Accepted: 09 July 2026; Published: 19 August 2026*

**Abstract:** This paper proposes a State of Health (SOH)–aware power management framework for a hybrid renewable energy system integrating solar photovoltaic, wind energy, and battery energy storage systems. Unlike conventional strategies that rely solely on State of Charge, the proposed approach embeds SOH as an active control variable within the power management algorithm to adapt battery dispatch based on degradation state. Real-world solar and wind datasets, along with experimentally obtained battery degradation data, are used for system evaluation. Simulation results demonstrate that incorporating SOH reduces battery stress, limits excessive cycling under degraded conditions, and improves long-term system reliability. The proposed framework enables lifecycle-aware energy management, enhancing the sustainability and operational resilience of hybrid renewable energy systems.



## Nomenclature

| | |
|---|---|
| SOC | State of Charge |
| SOH | State of Health |
| SPV | Solar Photovoltaic |
| WES | Wind Energy System |
| BESS | Battery Energy Storage System |
| PMA | Power Management Algorithm |
| HRES | Hybrid Renewable Energy System |
| GPR | Gaussian Process Regression |

**How to cite this article:** Joshi, Siddharth; Barva, Akash V.; Shah, Digesh D.. Integration of state of health in power management algorithms for hybrid renewable energy systems. *Transactions on Energy Systems and Engineering Applications*, 7(2): 860, 2026. DOI:10.32397/tesea.vol7.n2.860

| | |
|---|---|
| LSTM | Long Short-Term Memory |
| kW | kilowatt |
| W/m$^2$ | watt per square meter |
| m/s | meters per second |
| Ah | ampere-hour |

## 1. Introduction

Hybrid Renewable Energy Systems (HRES), which integrate Solar Photovoltaic (SPV), Wind Energy Systems (WES), and Battery Energy Storage Systems (BESS), have emerged as an effective and sustainable solution for reliable electricity supply, particularly in regions where access to the conventional grid is limited or unavailable [1–3]. These systems leverage the complementary nature of renewable sources, such as solar and wind, to stabilize power generation, addressing intermittent supply issues. BESS play a pivotal role in HRES by storing excess energy generated during peak renewable output and delivering it when generation is low, thus maintaining a continuous and reliable power supply [4,5]. However, the performance and efficiency of HRES heavily rely on the performance of BESS. Over time, batteries undergo degradation, primarily caused by factors such as charge-discharge cycles, temperature variations, and operational stresses, leading to a decline in storage capacity and discharge efficiency [6–8]. As batteries degrade, they lose their ability to store and release energy efficiently, directly impacting the overall performance of HRES. Therefore, accurately estimating the State of Health (SOH) of batteries becomes critical for predicting the remaining useful life of the energy storage system and ensuring optimal operation within HRES. SOH, typically expressed as the ratio of current battery capacity to initial capacity, serves as a crucial metric to monitor battery performance over time, helping prevent system failures and optimizing battery usage [9, 10]. While the integration of renewable energy sources mitigates intermittency challenges in HRES, dynamic operational conditions such as changing weather patterns and fluctuating energy consumption demand add complexity to the management of battery health. These variations necessitate the development of adaptive, accurate SOH estimation models that can adjust in real-time to the degradation of battery performance. This evolving challenge requires innovative solutions that incorporate SOH estimation into Power Management Algorithms (PMA) to optimize system operation, enhance battery life, and ensure a reliable power supply.

Recent advancements in HRES power management and SOH estimation have focused on improving system performance and extending the lifespan of BESS. Several studies have explored various techniques for battery management and optimization within microgrids. For instance, Shyni R. et al. [11] proposed an advanced framework for power management in standalone DC microgrids that incorporated SPV, WES, BESS, and Super Capacitors (SC), utilizing deep reinforcement learning to regulate state of charge (SOC) and DC voltage. However, this study did not address SOH factor, focusing primarily on voltage regulation. Similarly, W. Merrouche et al. [12] introduced an improved SOH model for batteries used in SPV, accounting for factors like battery aging and temperature. However, their approach remains limited to standalone solar systems, without considering multi-source integration, which is critical for HRES applications. M.H. Elkholy et al. [13] explored AI-based optimization in home energy management systems for microgrids but did not incorporate SOH or account for battery degradation. Suresh G. et al. [14] proposed a hybrid optimization method for smart grid power flow management incorporating SPV, WES, BESS, Fuel Cells (FC), and Diesel Generators (DG), but this study lacked any focus on SOH, further limiting the consideration of BESS performance. Xiaofen Fang et al. [15] developed an optimized multi-head self-attention mechanism for SOH factor in lithium-ion batteries within microgrids. While effective in estimating SOH under constant current and voltage charging modes, this method did not integrate SOH estimation with power management strategies, leaving a gap in battery health optimization.

Existing power management strategies for hybrid renewable energy systems predominantly rely on SOC as the primary indicator of battery availability and dispatch capability. Such approaches implicitly assume constant battery capacity and power delivery characteristics throughout the operational lifetime, which becomes increasingly inaccurate as battery degradation progresses. Although several studies have independently addressed power management or SOH estimation, the explicit integration of SOH into real-time operational decision-making remains largely unexplored. The key novelty of this work lies in embedding SOH as an active control variable within the PMA of a hybrid renewable energy system. Unlike conventional SOC-based or optimization-only frameworks, the proposed SOH-aware PMA dynamically adjusts battery dispatch, effective usable capacity, and depth-of-discharge limits based on the degradation state of the battery. As SOH declines, the algorithm progressively reduces battery utilization and adaptively reallocates power among renewable sources and grid support to prevent accelerated aging. By directly linking battery health estimation with operational power management, this study bridges a critical gap between battery degradation modeling and system-level energy management. This integration enables lifecycle-aware control, enhances long-term system reliability, extends battery lifespan, and improves overall sustainability—features that are not explicitly addressed in existing methodologies. While several studies have independently addressed power management optimization or battery SOH estimation, most existing frameworks assume constant battery capacity during real-time dispatch decisions. In contrast, the proposed framework establishes an explicit dynamic coupling between SOH estimation and dispatch control. The battery's allowable power limits, effective usable capacity, and SOC operating window are continuously adjusted as functions of real-time SOH. This degradation-aware adaptive control mechanism distinguishes the proposed strategy from conventional SOC-based or optimization-only approaches and enhances lifecycle-aware energy management within hybrid renewable energy systems.

The specific technical contributions of this work are summarized as follows:

- A novel SOH-aware power management framework is proposed in which battery State of Health is embedded as a real-time control variable, directly influencing dispatch priority, effective usable capacity, and depth-of-discharge limits.
- A degradation-adaptive PMA is developed that dynamically reallocates power among SPV, WES, BESS, and grid sources based on SOH evolution, preventing excessive cycling of degraded batteries.
- The impact of SOH decline on battery utilization, SOC behavior, and system-level power sharing is quantitatively analyzed using real-world renewable resource data and experimental battery degradation datasets.
- Comparative SOH prediction using GPR and LSTM models is performed to support reliable health-aware operational decision-making within hybrid renewable energy systems.

Despite extensive research on hybrid renewable energy systems, most existing studies focus either on short-term power management objectives such as load balancing and SOC regulation, or on battery health estimation as a standalone problem. The lack of coordination between SOH estimation and real-time operational control leads to battery dispatch decisions that ignore degradation effects, resulting in suboptimal utilization and accelerated aging. This gap highlights the need for a unified framework that links battery health awareness with system-level power management. Accordingly, the objectives of this study are: (i) to develop an SOH-aware power management algorithm that dynamically adapts battery dispatch based on degradation state, (ii) to analyze the impact of SOH decline on battery utilization and overall system performance, and (iii) to validate the proposed approach using real-world renewable resource data and experimentally obtained battery degradation datasets. Based on the identified research gap and defined objectives, the following section presents the system configuration and the proposed SOH-integrated power management methodology adopted for this study.

The paper is structured as follows: Section 1 provides an introduction to the study. Section 2 outlines the system configuration and methodology adopted for the analysis. Section 3 presents the results and discussion, highlighting key insights and observations. Finally, Section 4 concludes the study by summarizing the findings and their implications.

**Table 1.** Comparative review of existing power management and SOH estimation approaches in hybrid renewable energy systems.

| Ref. | System Type (SAS/ HRES) | System Configuration | PMA | SOH Estimation | SOH Factor Consideration | Integration with HRES | Remarks |
|---|---|---|---|---|---|---|---|
| [11] | SAS | SPV, WES, BESS, and SC | ✓ | * | * | * | • Demonstrates robust control of SOC and DC voltage.<br>• Implements deep reinforcement learning for PMA under varying renewable generation.<br>• Excludes SOH considerations for BESS health. |
| [12] | SAS | SPV, and BESS | * | ✓ | ✓ | * | • Proposes an improvement of a previous SOH model based on working zone and temperature.<br>• Relies on PV designer software and test equipment accuracy.<br>• Limited to standalone solar systems. |
| [13] | HRES | SPV, WES, and BESS | ✓ | * | * | ✓ | • Focuses on optimizing microgrid performance by integrating power limitations.<br>• Effectively balances multi-source power flow.<br>• Does not address battery SOH factor of BESS. |
| [14] | HRES | SPV, WES, BESS, FC and DG | ✓ | * | * | ✓ | • Aims to reduce costs and control power flow in the system.<br>• Uses power and capacity constraints in optimization.<br>• Does not consider battery health parameter. |
| [15] | HRES | SPV, WES, and BESS | * | ✓ | ✓ | ✓ | • Uses CC and CV charging modes for SOH estimation.<br>• Implements multi-head self-attention to manage multiple lithium batteries.<br>• Does not analyze power management in relation to battery health. |
| This Work | HRES | SPV, WES, and BESS | ✓ | ✓ | ✓ | ✓ | • Proposes integrating SOH into HRES power management to enhance system performance.<br>• Reduces battery stress, extending lifespan and minimizing replacement needs.<br>• Strengthens system resilience by adapting to energy demand and renewable fluctuations. |

## 2. System Configuration and Methodology

This section outlines the methodology used to simulate the operation of a HRES and estimate the SOH of the BESS within the context of power management algorithm. The proposed approach combines solar and wind energy generation with a battery storage system and integrates the SOH estimation for optimal energy flow management. The methodology also describes the integration of real-time data, the simulation setup, and the power management algorithm.

### 2.1. System Configuration and Data Collection

The HRES considered in this study integrates three key components: SPV, WES, and BESS. These components are designed to provide a reliable and sustainable power supply, particularly in areas where access to a conventional power grid is limited. The SPV system utilizes Adani Multi-crystalline Solar PV Modules (ASP-7-AAA) [16], each with a rated power of 320 Wp. The system configuration consists of 50 kW of solar capacity, achieved by combining multiple strings of modules connected in series. The output from the SPV is directly affected by solar irradiance, which is influenced by local weather conditions. The solar power generation is dynamically adjusted to real-time solar irradiance data, which is sourced from historical records using PVlib's PVGIS-TMY data for the Gujarat region [17,18]. The Endurance E-3120 50 kW Wind Turbine [19] is employed for wind energy generation. This system operates with a rotor diameter of 19 m and is rated to produce 50 kW under optimal wind conditions. The wind power generated is modeled using historical wind speed data, where the power output is estimated using the cubic relationship of wind speed in the range of 3–25 m/s. Real-time wind speed data is integrated into the simulation for accurate power generation forecasts [20]. Solar irradiance (in W/m$^2$) and wind speed (in m/s) data are collected from the PVGIS TMY dataset provided by PVlib for the Gujarat region – Western region, India. The data includes historical records of solar radiation and wind speed, which are used to simulate solar and wind power generation throughout the day. These time-series datasets offer essential insights into the available renewable resources, ensuring that the simulation reflects real-world conditions. The BESS is modeled with a rated capacity of 30 kWh, capable of charging and discharging between 10% and 90% SOC. The system is designed to smooth fluctuations in power generation by charging during surplus energy periods (high solar/wind output) and discharging during deficit periods (high demand/low generation). The BESS is crucial for stabilizing the power supply from intermittent renewable sources. The degradation of the BESS is tracked via SOH, which is simulated based on the charging and discharging cycles. The NASA Battery Dataset (B0005, B0006, B0007, B0018 and B0045, B0046, B0047, B0048) is employed to estimate the SOH of the BESS [21]. In this study B0047 dataset considered. This dataset includes measurements of voltage, current, and temperature over time, which are crucial for tracking the battery's degradation during charge/discharge cycles.

The effectiveness of the proposed SOH-aware power management strategy is validated through detailed simulation studies using real-world datasets. Solar irradiance and wind speed profiles are obtained from the PVGIS Typical Meteorological Year (TMY) database for the Gujarat region, ensuring realistic renewable generation patterns. Battery degradation behavior is modeled using experimentally measured data from the NASA lithium-ion battery dataset (B0047), which provides voltage, current, temperature, and capacity measurements over multiple charge–discharge cycles. These datasets enable reproducible evaluation of system performance under practical operating conditions. It is important to note that the PVGIS TMY dataset does not represent a single historical day but rather a statistically constructed annual profile derived from long-term meteorological measurements. The TMY approach ensures that renewable generation patterns reflect representative climatic behavior for the selected region. Therefore, the simulation results are based on climatologically averaged renewable resource conditions rather than isolated short-term measurements.

Although the proposed power management algorithm follows a rule-based supervisory structure, its novelty lies in the explicit integration of degradation-aware adaptive constraints within the dispatch logic. Conventional rule-based controllers operate with fixed SOC thresholds and constant power limits throughout battery lifetime. In contrast, the proposed approach dynamically modifies battery power capability, effective energy capacity, and SOC operating window as explicit functions of real-time SOH. This transforms the controller from a static logic framework into a lifecycle-aware adaptive dispatch mechanism. The rule-based architecture is intentionally retained to ensure transparency, computational efficiency, and suitability for real-time microgrid implementation while embedding degradation-aware intelligence within operational decisions.

### 2.2. Power Management Algorithm

A power management strategy is implemented to control the flow of energy within the HRES, ensuring optimal operation of the SPV, WES, BESS, and the grid. The algorithm follows a mode-based control system that considers different operational states: When the available renewable power exceeds the load demand, the excess energy is used to charge the battery. This mode ensures that the battery SOC does not exceed the maximum threshold. If renewable power generation is insufficient to meet the load, the system discharges the battery to supply the deficit. The SOC is monitored to prevent over-discharge. In cases where the SOC is outside the acceptable range (below 10% or above 90%), the battery is isolated from the system to avoid degradation due to overcharging or excessive discharge. The algorithm dynamically adjusts the energy flow based on real-time conditions, ensuring that the battery remains within the optimal operating range and minimizes the impact of SOH degradation.

The proposed power management algorithm adopts a rule-based, mode-driven structure due to its transparency, low computational burden, and suitability for real-time implementation in hybrid renewable energy systems. This structure allows explicit inclusion of SOH-dependent constraints within the decision logic, which is difficult to achieve using black-box optimization techniques. The PMA continuously adapts to varying operating conditions by monitoring renewable generation, load demand, SOC, and SOH. As renewable availability or battery health changes, the algorithm dynamically adjusts battery dispatch priority, depth-of-discharge limits, and grid support to ensure safe and reliable system operation.

#### 2.2.1. Mathematical Formulation of SOH-Aware Power Management

To explicitly demonstrate the operational integration of SOH within the proposed framework, the power management algorithm is mathematically formulated. Unlike conventional SOC-based strategies that assume constant battery capacity and power limits, the proposed formulation treats SOH as a dynamic system state that directly modifies dispatch constraints, effective capacity, and operating boundaries.

At each time step $t$, system power balance is maintained as:

$$P_{SPV}(t) + P_{WES}(t) + P_{BESS}(t) + P_{grid}(t) = P_{load}(t), \tag{1}$$

where $P_{SPV}$, $P_{WES}$, $P_{BESS}$, $P_{grid}$, and $P_{load}$ represent solar, wind, battery, grid, and load power contributions, respectively.

The effective battery energy capacity is modeled as:

$$E_{eff}(t) = SOH(t) \times E_{rated}, \tag{2}$$

where $E_{rated}$ is the nominal battery capacity. As SOH decreases due to aging, the usable energy storage capacity proportionally reduces.

The SOC evolution is computed as:

$$SOC(t+1) = SOC(t) + \frac{\eta_{ch} P_{ch}(t) - \dfrac{P_{dis}(t)}{\eta_{dis}}}{E_{eff}(t)}, \tag{3}$$

where $\eta_{ch}$ and $\eta_{dis}$ denote charging and discharging efficiencies, and $P_{ch}(t)$ and $P_{dis}(t)$ represent charging and discharging power. By incorporating $E_{eff}(t)$, the SOC calculation inherently reflects degradation effects.

To prevent excessive stress on degraded batteries, the maximum allowable charge and discharge power are adaptively reduced:

$$P_{BESS}^{max}(t) = SOH(t) \times P_{rated}, \tag{4}$$

subject to:

$$P_{BESS}(t) \leq P_{BESS}^{max}(t). \tag{5}$$

This ensures degraded batteries are not operated at nominal power ratings.

To further mitigate accelerated aging under degraded conditions, the SOC limits are dynamically adjusted:

$$SoC_{min}(t) = SoC_{min}^{nominal} + \alpha \left(1 - SOH(t)\right), \tag{6}$$

$$SoC_{max}(t) = SoC_{max}^{nominal} - \beta \left(1 - SOH(t)\right), \tag{7}$$

where $\alpha$ and $\beta$ are degradation sensitivity coefficients, and $SoC_{min}^{nominal}$ and $SoC_{max}^{nominal}$ are standard operating limits (10%–90%). As SOH declines, the allowable SOC range narrows, reducing depth-of-discharge and cycling stress.

To ensure closed-loop coupling between battery usage and health degradation, SOH is updated at each simulation step as:

$$SOH(t+1) = SOH(t) - \Delta SOH(t), \tag{8}$$

where the degradation increment is modeled as:

$$\Delta SOH(t) = k_1.DoD(t) + k_2.|C - rate(t)| \tag{9}$$

where $DoD(t)$ is depth-of-discharge, $C\text{-}rate(t)$ represents normalized current stress, and $k_1$ and $k_2$ are empirical degradation coefficients. This formulation ensures that deeper cycling and higher charge/discharge rates accelerate degradation, establishing a dynamic interaction between operational stress and long-term battery health.

Through this formulation, SOH directly influences effective energy capacity, maximum dispatchable power, SOC operating limits, and long-term feasibility of battery utilization. Therefore, SOH functions as an active control variable embedded within real-time power management rather than a passive diagnostic parameter.

The proposed formulation establishes a bidirectional interaction between battery operation and degradation dynamics. At each time step, the current SOH value modifies effective energy capacity, allowable charge/discharge power limits, and the SOC operating window within the PMA. The resulting dispatch decisions determine operational stress indicators such as depth-of-discharge (DoD) and C-rate. These stress variables directly influence the subsequent degradation increment $\Delta SOH(t)$, thereby updating the SOH for the next time step. Consequently, battery usage at time step $t$ affects SOH at time step $t+1$, and the updated SOH subsequently modifies future dispatch feasibility. This closed-loop interaction ensures that SOH is treated as a dynamic system state embedded within real-time control rather than a static external parameter.

### *2.3. SOH Analysis*

The SOH is a key parameter for understanding the battery's ability to store and discharge energy efficiently. SOH is calculated based on the battery's charge/discharge cycles, temperature, and voltage characteristics. Over time, as the battery undergoes charge and discharge cycles, its capacity gradually decreases, which is reflected in the SOH. In this study, simplified degradation models are employed, where SOH is reduced by a fixed percentage during discharge cycles and slightly improved during charge cycles. For improved prediction accuracy, data-driven machine learning techniques are employed to estimate SOH based on the historical performance of the battery. Error metrics like Mean Absolute Percentage Error (MAPE) and Root Mean Square Error (RMSE) are used to evaluate the accuracy of the SOH prediction model. These metrics compare the predicted SOH against the actual measurements in the NASA dataset. The model's accuracy is validated by comparing the simulated SOH with actual data from the NASA battery dataset. Performance metrics, such as MAPE and RMSE, are computed to quantify the error in SOH estimation. In this study, a reduction in error is aimed for through iterative adjustments in the power management and SOH estimation models. Additionally, the predicted SOH is used to simulate the potential impact of battery degradation on power management. As the SOH decreases, the battery's ability to store energy reduces, leading to more frequent reliance on grid power or more significant power shortages. Therefore, incorporating SOH prediction into the power management strategy is crucial to improving the system's efficiency, reducing operational costs, and enhancing the sustainability of the HRES.

The SOH estimation approach is selected based on its ability to capture non-linear battery degradation behavior using experimentally validated data. The NASA B0047 lithium-ion battery dataset is employed due to its comprehensive cycle-life measurements, making it suitable for reproducible degradation analysis. Gaussian Process Regression (GPR) is used for SOH prediction owing to its robustness with limited training data and uncertainty handling, while Long Short-Term Memory (LSTM) networks are included for comparative evaluation of temporal learning capability. These models enable adaptive system operation by providing real-time SOH information to the power management algorithm. The proposed system configuration, power management algorithm, and SOH estimation framework are evaluated in the following section through detailed simulation studies to analyze system performance under varying operating conditions.

To ensure clarity and methodological consistency, the SOH estimation process adopted in this study is structured into three stages: (i) dataset preparation, (ii) model training and comparative evaluation, and (iii) integration into the SOH-aware power management algorithm.

#### 2.3.1. Dataset Description

The NASA lithium-ion battery dataset (B0047) is selected due to its experimentally validated cycle-life characterization under controlled laboratory conditions. The dataset includes voltage, current, temperature, and discharge capacity measurements over multiple charge–discharge cycles. The nominal initial capacity of the battery is 1.855 Ah, with End-of-Life (EOL) defined at 70% SOH.

SOH is computed as:

$$SOH = \frac{C_{measured}}{C_{initial}}, \tag{10}$$

where $C_{measured}$ represents the discharge capacity at a given cycle and $C_{initial}$ denotes the initial rated capacity.

#### 2.3.2. Machine Learning Model Comparison

To accurately predict SOH degradation, two data-driven machine learning models were implemented and evaluated: Gaussian Process Regression (GPR) and Long Short-Term Memory (LSTM).

Both models were trained using cycle number and electrochemical features (voltage, current, and temperature) as input variables. Model performance was evaluated using: Mean Absolute Percentage Error (MAPE), Mean Absolute Error (MAE), and Root Mean Square Error (RMSE).

The comparative analysis demonstrated that the GPR model achieved lower prediction errors and smoother long-term degradation tracking compared to LSTM. Therefore, GPR was selected as the primary SOH estimation model for integration into the SOH-aware PMA.

#### 2.3.3. Real-Time SOH Integration into PMA

The real-time SOH estimation is expressed as:

$$SOH(t) = f_{GPR}\left(V(t), I(t), T(t), Cycle(t)\right). \tag{11}$$

The predicted SOH value is updated at each simulation step and directly transmitted to the power management algorithm. This establishes a closed-loop coupling between battery degradation estimation and operational dispatch decisions.

LSTM results are retained for comparative validation and benchmarking purposes but are not embedded within the operational control loop.

## 3. Results and Discussion

This section presents the simulation results of the proposed HRES, which integrates SPV, WES, and BESS. The performance of the system is analyzed over a 24-hour period using real-time data for solar irradiance and wind speed. The impact of battery degradation, represented by the SOH, on system performance is also assessed. The study evaluates the power generation capabilities, load management, and the effectiveness of the power management algorithm. The simulation studies are conducted over a 24-hour operational horizon to evaluate the proposed SOH-integrated power management framework under varying renewable generation, load demand, and battery health conditions. System performance is assessed using key evaluation metrics including battery utilization, State of Charge (SOC) evolution, power sharing among sources, and SOH prediction accuracy quantified using Mean Absolute Percentage Error (MAPE), Mean Absolute Error (MAE), and Root Mean Square Error (RMSE). These metrics collectively demonstrate the impact of SOH-aware control on system reliability and battery lifespan.

### *3.1. Power Generation and Load Demand*

The primary objective of the HRES is to utilize renewable energy sources to meet the load demand while ensuring efficient energy management. The SPV and WES are modeled to generate power based on real-time solar irradiance and wind speed data obtained from the PVGIS-TMY dataset. The load demand is met by combining renewable energy generation and battery storage, with the grid acting as a backup source.

Figure 1 illustrates the power generation from SPV, WES, and the total load demand. The solar power generation follows the irradiance curve and peaks during daylight hours. Wind power generation exhibits fluctuations, reflecting the variability in wind speeds throughout the day. From the results, it is evident that during daytime hours, solar power contributes significantly to meeting the load demand, reducing the reliance on wind power and the BESS. In the evening, as solar power declines, wind power and the BESS play a critical role in maintaining energy supply.

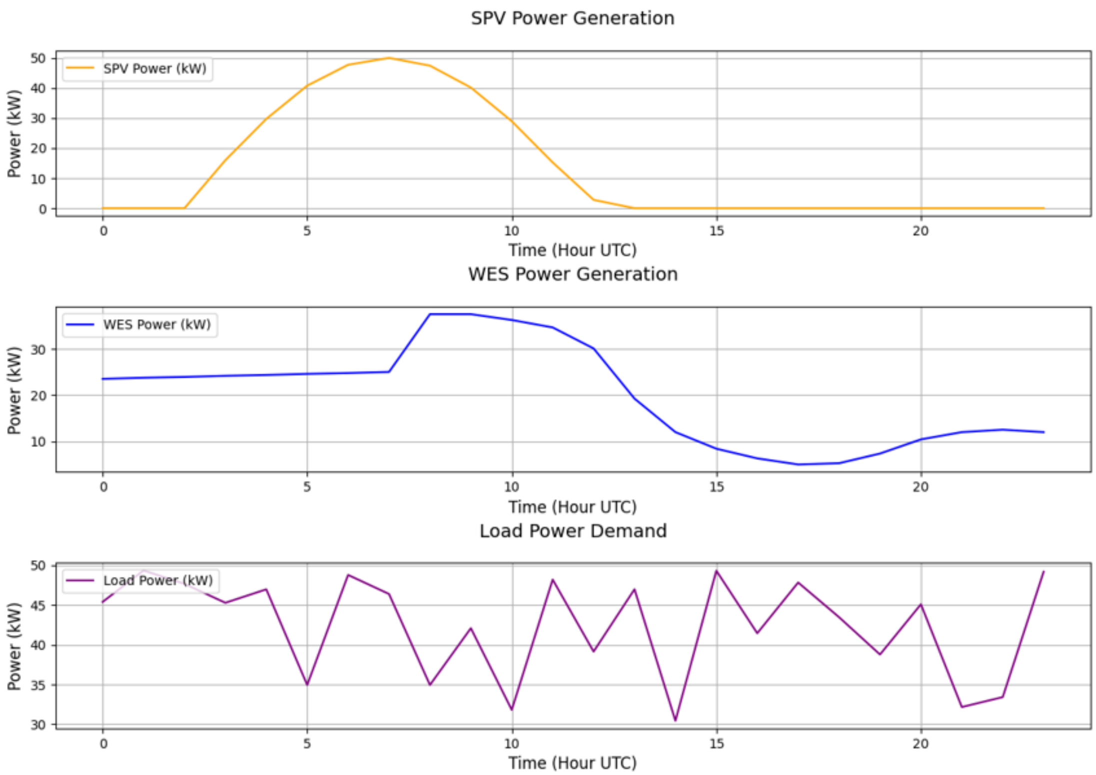


**Figure 1.** Power generation from SPV and WES in comparison with load demand over a 24-hour operating period.

Solar energy generation is modeled using the Adani ASP-7-AAA panels, with a total capacity of 50 kW. The power output closely follows the irradiance curve, as shown in Figure 2, peaking during midday. Wind energy generation is based on the Endurance E-3120 wind turbine's power curve, interpolating power output for wind speeds between 0 and 25 m/s. Figure 2 illustrates wind speed and the corresponding power generation. The results highlight the complementarity of solar and wind energy sources. During periods of low solar irradiance, wind power compensates, and vice versa, ensuring a balanced energy supply throughout the day.

The BESS stabilizes the HRES by storing surplus energy during high renewable generation periods and discharging it during deficits. Figure 3 shows the hourly variations in SOC over the simulation period. The SOC values remain within the operational range of 10% to 90%, reflecting the effectiveness of the power management algorithm in preserving battery health and optimizing usage. The BESS charges during daylight hours when renewable generation exceeds the load and discharges during the evening, compensating for reduced SPV output.

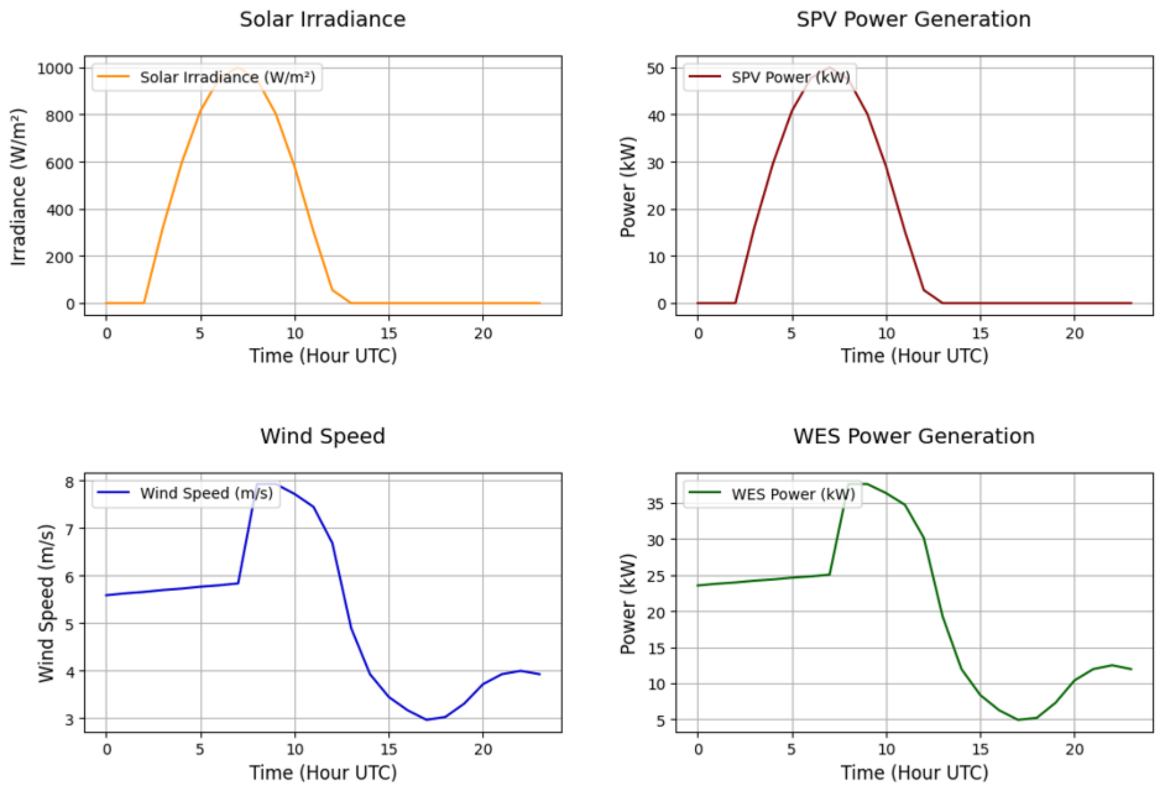


**Figure 2.** Solar irradiance and wind speed profiles with corresponding SPV and WES power generation.

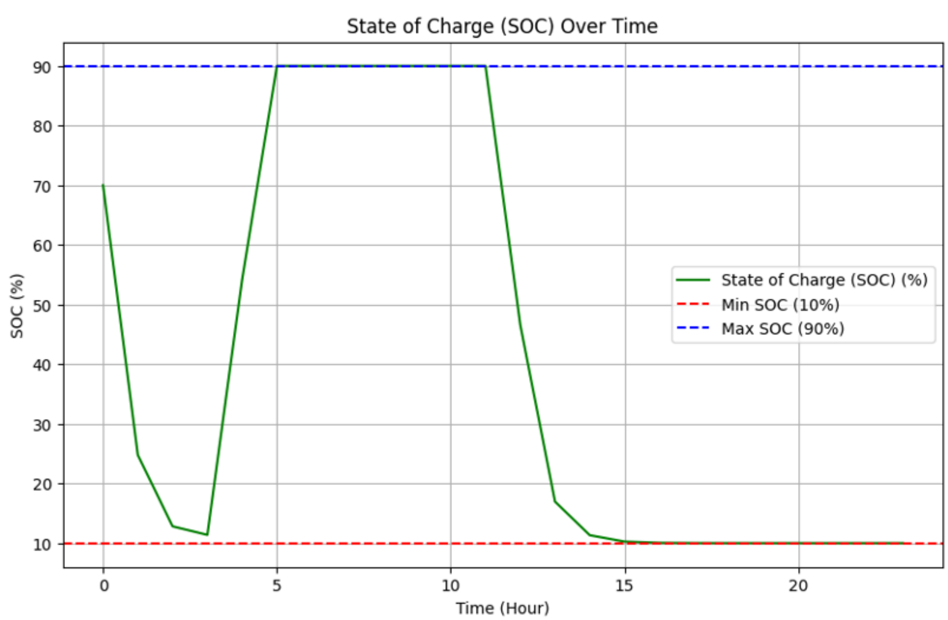


**Figure 3.** State of Charge (SOC) variation of the battery energy storage system under SOH-aware power management.

### *3.2. SOH Degradation Analysis*

The analysis of SOH degradation plays a crucial role in assessing the long-term viability and performance of batteries, particularly in energy storage systems. In this study, we focus on the degradation behavior of the NASA B0047 battery, a lithium-ion cell with $LiNi_{0.8}Co_{0.15}Al_{0.05}O_2$ (NCA) chemistry, which is widely used in various applications due to its high energy density and stability. SOH is an indicator of the battery's overall health, defined as the ratio of the battery's current capacity to its initial nominal capacity. For the NASA B0047 battery, the initial nominal capacity is 1.855 Ah, and the End of Life (EOL) is typically considered at 70% SOH, corresponding to a capacity of 1.298 Ah. The battery undergoes charge and discharge cycles, and its degradation is tracked over multiple cycles. In this analysis, the actual SOH values are derived from the capacity measurements taken during each discharge cycle. These actual SOH values are compared against predicted SOH values generated by models that capture the degradation trends. Specifically, we evaluate the prediction performance of two models: the Gaussian Process Regressor (GPR) and Long Short-Term Memory (LSTM). Both models were trained on the cycle number and corresponding SOH data to estimate future SOH degradation. The results reveal the deviations between the actual and predicted SOH values, offering insights into the models' accuracy in replicating the battery's real-world degradation. The performance of these models was evaluated using three error metrics: Mean Absolute Percentage Error (MAPE), Mean Absolute Error (MAE), and Root Mean Squared Error (RMSE). The results are summarized in Table 2 below:

**Table 2.** Performance comparison of GPR and LSTM models for SOH prediction using the NASA B0047 battery dataset.

| Model | MAPE (%) | MAE (%) | RMSE (%) |
|---|---|---|---|
| GPR | 0.58 | 0.41 | 0.59 |
| LSTM | 1.07 | 0.74 | 1.09 |

In particular, the Gaussian Process Regressor (GPR) model demonstrated a strong performance with an average Mean Absolute Error (MAE) of 0.279%, indicating that it closely follows the actual degradation trend. In contrast, the Long Short-Term Memory (LSTM) model had a slightly higher MAE of 1.096%, which is still within acceptable limits but suggests that the model may require further optimization to improve its predictions. Overall, the analysis underscores the importance of accurate SOH prediction in battery management systems, highlighting the strengths and limitations of each model in predicting long-term performance. It also identifies opportunities for refining the models to enhance their predictive capabilities, ensuring better monitoring and forecasting of battery health in real-world applications.

Figure 4 illustrates the comparison between actual SOH degradation and the predicted SOH obtained using GPR and LSTM models. The GPR model demonstrates closer alignment with the experimental degradation trend, exhibiting lower prediction error and smoother convergence over cycling. This improved accuracy is reflected in the reduced MAPE, MAE, and RMSE values reported in Table 2, indicating that GPR is more suitable for long-term SOH tracking in power management applications where reliable degradation awareness is critical.

The dynamically estimated SOH values are subsequently integrated into the SOH-aware PMA, establishing a feedback mechanism between battery usage and long-term degradation. Increased cycling intensity or deeper discharge events accelerate degradation, which in turn reduces allowable battery dispatch limits in subsequent time steps. This feedback interaction demonstrates the dynamic coupling between degradation estimation and operational control within the proposed framework.

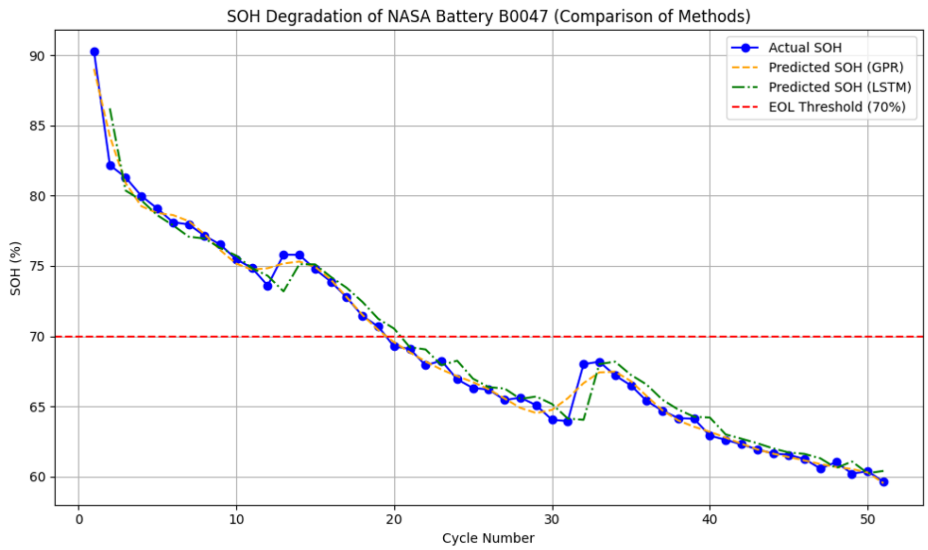


**Figure 4.** Comparison of actual and predicted SOH degradation using GPR and LSTM models.

### *3.3. Impact of SOH on PMA in HRES*

Beyond proportional capacity scaling, SOH directly modifies dispatch feasibility and energy allocation priority within the proposed PMA. As SOH declines, three operational adaptations occur: (A) The maximum allowable battery power is reduced, limiting aggressive charge–discharge behavior; (B) The SOC operating window narrows, preventing deep cycling under degraded conditions; and (C) Grid support is progressively prioritized when battery dispatch constraints are reached. This multi-layered influence ensures that SOH affects not only available storage energy but also real-time power sharing decisions and overall system reliability. Therefore, SOH operates as a dynamic operational constraint rather than merely a health indicator.

In addition to the dynamic SOH evolution described in Section 2.2.1, fixed-SOH scenarios (100%, 90%, 80%, and 70%) are presented to isolate the influence of degradation severity on dispatch behavior. These scenarios serve as controlled sensitivity analyses. However, within the closed-loop simulation framework, SOH is continuously updated based on operational stress, enabling progressive degradation modeling under real-time system operation. This distinction ensures both comparative evaluation and dynamic degradation-aware dispatch integration.

The integration of SOH into PMA strategies in HRES plays a critical role in optimizing the operational efficiency, longevity, and economic performance of energy storage devices, particularly batteries. As SOH deteriorates, the performance and capacity of the battery are directly impacted, altering the energy flow within the system. This section explores the impact of SOH degradation on PMA in HRES, highlighting how system performance is optimized in response to changes in battery health. In the proposed framework, State of Health (SOH) directly influences power management decisions by modifying the effective usable capacity and discharge capability of the battery energy storage system. The PMA continuously receives updated SOH values and proportionally derates battery dispatch as degradation progresses. At lower SOH levels, the algorithm limits battery discharge power and depth-of-discharge, while prioritizing renewable generation and grid support to satisfy load demand. This SOH-driven adaptation ensures that battery utilization reflects actual degradation conditions rather than nominal capacity assumptions. Consequently, the PMA prevents excessive cycling of degraded batteries, reduces aging acceleration, and maintains system reliability under varying operating conditions—capabilities not achievable using conventional SOC-only control strategies.

### 3.3.1. Battery Utilization and System Performance in Relation to SOH

In this study, the method employed for predicting battery power and SOC based on different SOH levels involves dynamically adjusting the effective battery capacity according to the SOH percentage. Specifically, the nominal capacity of the 30 kWh battery is scaled by the SOH level (e.g., 100%, 90%, 80%, and 70%) to simulate the reduced storage capability as the SOH decreases. The simulation considers both the surplus and deficit power scenarios from the SPV and WES, and updates the SOC hourly, factoring in charging and discharging efficiencies of 95% and 90%, respectively. The SOC is constrained within the defined limits of 10% to 90% to avoid overcharging or deep discharge. At full health, the battery operates at its maximum capacity, providing optimal charge and discharge rates without compromising its lifespan. This allows the energy management system to rely heavily on the battery for storing excess renewable energy during periods of overproduction, and for discharging during periods of high demand or insufficient renewable generation. However, as SOH decreases due to aging or extensive cycling, the effective storage capacity of the battery declines. This reduces the battery's ability to store energy and limits its role in the power management strategy, leading to changes in how power is distributed across the system. Figure 5 shows SOH impact on battery utilization. Appendix 1 illustrates the influence of the SOH on battery utilization and overall system performance. At 100% SOH, the battery demonstrates optimal discharge capabilities, contributing significantly to meeting the load demand by compensating for gaps in renewable energy supply. As SOH decreases, a marked reduction in battery power is observed, particularly during peak demand hours, which necessitates greater reliance on grid power. This trend is evident in Hour 1, where battery power at 100% SOH is 20 kW, dropping to 14 kW at 70% SOH.

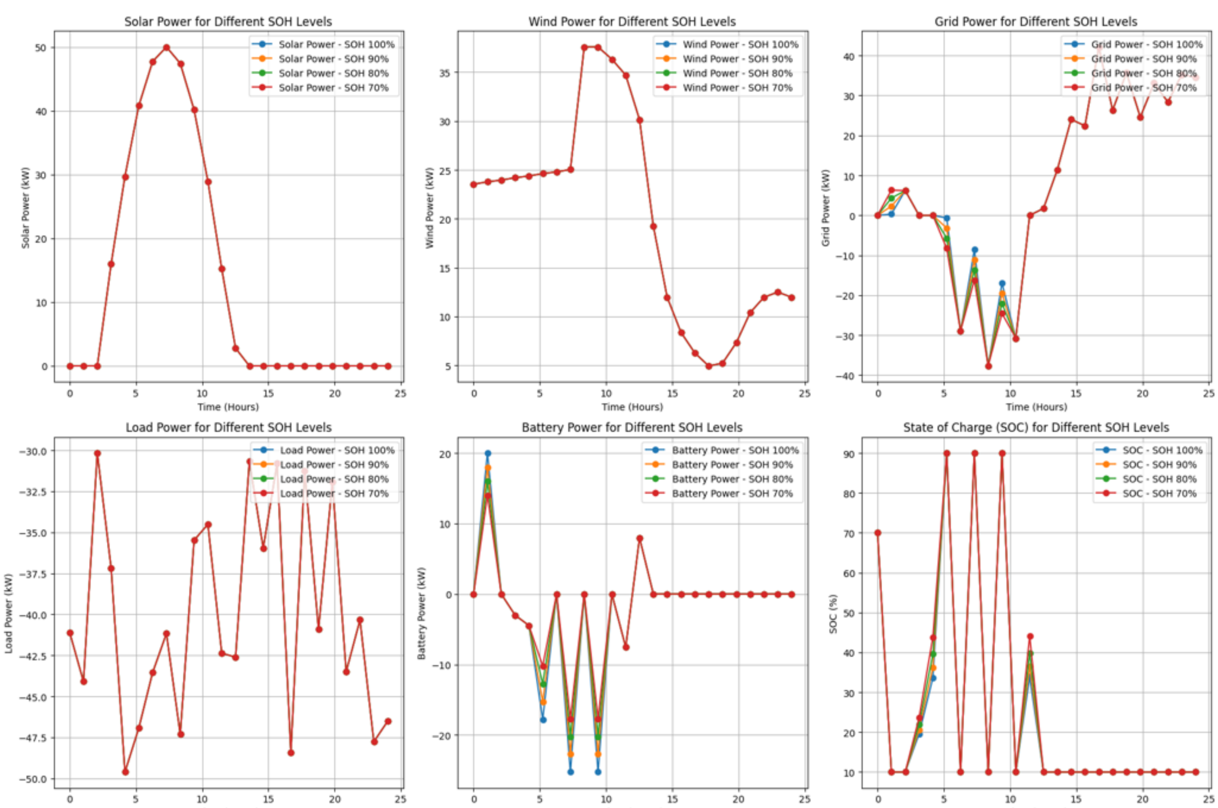


**Figure 5.** Impact of State of Health (SOH) degradation on battery discharge contribution in the proposed HRES.

Similarly, the SOC is better maintained at higher SOH levels, ensuring system flexibility and reliability. These observations underscore the critical role of SOH in determining the efficiency and resilience of hybrid renewable energy systems.

Figure 5 highlights the direct impact of SOH degradation on battery utilization within the hybrid renewable energy system. As SOH decreases from 100% to 70%, a progressive reduction in battery discharge contribution is observed, particularly during high load demand periods. This trend confirms the effectiveness of the proposed SOH-aware PMA, which adaptively limits battery usage under degraded conditions and compensates through renewable generation and grid support, thereby reducing battery stress while maintaining system stability.

#### 3.3.2. System Adaptation to SOH Decline

As the battery health decreases, the PMA adapts by reducing reliance on the battery for energy storage. The system prioritizes renewable energy sources, such as solar or wind, to store energy and meet load demands, while reducing the depth of discharge (DoD) of the battery to slow its degradation. This helps in optimizing the overall energy efficiency and minimizing wear on the battery. Furthermore, when the battery is unable to meet the deficit between renewable generation and load consumption, grid power is used to ensure system stability. By dynamically adjusting the power distribution, PMA systems ensure that the energy storage system continues to support the hybrid microgrid even as battery performance deteriorates, without causing excessive wear or operational inefficiency. Conventional energy management strategies often overlook the dynamic impact of the SOH on battery performance. Decisions are typically based solely on power degradation, assuming that a given SOC will consistently provide the same power output. However, as SOH declines, this assumption becomes invalid since the effective capacity and power delivery capabilities of the battery are significantly reduced. This necessitates a redefinition of SOC thresholds to account for SOH variations, ensuring that power management strategies adapt to maintain the battery's operation within safe limits, prolonging its lifecycle and ensuring reliable system performance.

### *3.4. Discussion on Validation Scope and Generalizability*

The results presented in Sections 3.1–3.3 focus on a representative 24-hour operational cycle to clearly illustrate system behavior, power sharing dynamics, and SOH-aware dispatch adaptation. The proposed framework itself is formulated using time-recursive SOC and SOH evolution equations (Section 2.2.1), and therefore is not inherently restricted to a single-day horizon. The fixed SOH scenarios (100%, 90%, 80%, and 70%) provide controlled robustness analysis across different degradation states, demonstrating consistent degradation-aware behavior under varying health conditions. These sensitivity analyses offer insight into long-term operational adaptation without assuming constant battery capability. While the present study utilizes one publicly available lithium-ion dataset and one representative geographical renewable profile, the proposed SOH-aware dispatch framework is model-agnostic and can be extended to other battery chemistries and climatic regions provided appropriate SOH estimation models and renewable datasets are available.

## 4. Conclusion

The findings highlight the significance of integrating a HRES comprising SPV, WES, and BESS for sustainable energy applications. The study demonstrates how the complementary nature of SPV and WES reduces intermittency challenges, ensuring consistent power supply with minimal reliance on grid electricity. The combination of renewable sources and energy storage enhances system reliability while addressing fluctuations in energy demand. A key contribution of this research is the incorporation of battery SOH into the PMA, addressing a critical gap in conventional energy management systems. Traditional approaches primarily focus on the SOC without accounting for long-term battery degradation. By integrating SOH into the operational framework, the proposed system optimizes energy allocation, adapts to declining battery performance, and prolongs battery lifespan. The analysis reveals that SOH deterioration significantly affects storage capacity and discharge efficiency, underscoring the importance of real-time SOH monitoring for effective energy management. The research underscores the necessity of revisiting conventional PMA designs to account for non-linear relationships between SOC and power output, especially as batteries age. This adaptive approach ensures that energy systems remain resilient and capable of meeting demand under varying operational conditions. Moreover, the integration of predictive SOH analysis into HRES represents a transformative step toward more sustainable and economically viable renewable energy solutions. Although the validation is conducted using a representative renewable dataset and a widely benchmarked lithium-ion battery dataset, the present study is limited to simulation-based analysis under a specific regional climatic profile. Future work will extend the framework to multi-regional renewable datasets, additional battery chemistries, and long-term annual operational studies to further enhance generalizability and practical deployment readiness. Future advancements in dynamic power management strategies could explore the real-world implementation of these methodologies in larger-scale renewable energy systems. While the proposed SOH-aware power management framework demonstrates clear advantages in enhancing battery lifespan and system reliability, the present study is limited to simulation-based validation and a single battery chemistry. Practical implementation may involve additional challenges such as sensor inaccuracies, communication delays, and computational constraints in real-time controllers. Future work will focus on experimental validation through hardware-in-the-loop testing, extension to larger-scale hybrid systems with multiple battery units, and real-time deployment of the proposed PMA in practical microgrid environments.

**Funding:** This research received no external funding.

**Author contributions:** Conceptualization: Siddharth Joshi, Akash V. Barva; Methodology: Siddharth Joshi and Akash V. Barva; Software: Akash V. Barva; Validation: Siddharth Joshi, and Digesh D. Shah; Formal Analysis: Siddharth Joshi and Akash V. Barva; Investigation: Siddharth Joshi and Digesh D. Shah; Data Curation: Siddharth Joshi; Writing – Original Draft Preparation: Akash V. Barva; Writing – Review & Editing: Siddharth Joshi and Digesh D. Shah;

**Disclosure statement:** The authors declare no conflict of interest.

## Appendix 1

Hourly power sharing and battery utilization under different SOH levels in the hybrid renewable energy system.

**Table 3.** Hourly power sharing and battery utilization under different SOH levels.

| SOH (%) | Hour | SPV (kW) | WES (kW) | Grid (kW) | Load (kW) | BESS (kW) | SOC (%) |
|---|---|---|---|---|---|---|---|
| 100 | 1 | 0 | 24 | 1 | −45 | 20 | 10 |
| 90 | 1 | 0 | 24 | 3 | −45 | 18 | 10 |
| 80 | 1 | 0 | 24 | 5 | −45 | 16 | 10 |
| 70 | 1 | 0 | 24 | 7 | −45 | 14 | 10 |
| 100 | 2 | 0 | 24 | 18 | −42 | 0 | 10 |
| 90 | 2 | 0 | 24 | 18 | −42 | 0 | 10 |

*(continued on next page)*

*(continued from previous page)*

| SOH (%) | Hour | SPV (kW) | WES (kW) | Grid (kW) | Load (kW) | BESS (kW) | SOC (%) |
|---|---|---|---|---|---|---|---|
| 80 | 2 | 0 | 24 | 18 | −42 | 0 | 10 |
| 70 | 2 | 0 | 24 | 18 | −42 | 0 | 10 |
| 100 | 3 | 16 | 24 | 0 | −32 | −9 | 37 |
| 90 | 3 | 16 | 24 | 0 | −32 | −9 | 41 |
| 80 | 3 | 16 | 24 | 0 | −32 | −9 | 44 |
| 70 | 3 | 16 | 24 | 0 | −32 | −9 | 49 |
| 100 | 4 | 30 | 24 | 0 | −41 | −13 | 80 |
| 90 | 4 | 30 | 24 | 0 | −41 | −13 | 87 |
| 80 | 4 | 30 | 24 | −2 | −41 | −12 | 90 |
| 70 | 4 | 30 | 24 | −4 | −41 | −9 | 90 |
| 100 | 5 | 41 | 25 | −15 | −47 | −3 | 90 |
| 90 | 5 | 41 | 25 | −18 | −47 | −1 | 90 |
| 80 | 5 | 41 | 25 | −18 | −47 | 0 | 10 |
| 70 | 5 | 41 | 25 | −18 | −47 | 0 | 10 |
| 100 | 6 | 48 | 25 | −34 | −39 | 0 | 10 |
| 90 | 6 | 48 | 25 | −34 | −39 | 0 | 10 |
| 80 | 6 | 48 | 25 | −14 | −39 | −20 | 90 |
| 70 | 6 | 48 | 25 | −16 | −39 | −18 | 90 |
| 100 | 7 | 50 | 25 | −14 | −36 | −25 | 90 |
| 90 | 7 | 50 | 25 | −17 | −36 | −23 | 90 |
| 80 | 7 | 50 | 25 | −39 | −36 | 0 | 10 |
| 70 | 7 | 50 | 25 | −39 | −36 | 0 | 10 |
| 100 | 8 | 47 | 38 | −48 | −37 | 0 | 10 |
| 90 | 8 | 47 | 38 | −48 | −37 | 0 | 10 |
| 80 | 8 | 47 | 38 | −28 | −37 | −20 | 90 |
| 70 | 8 | 47 | 38 | −30 | −37 | −18 | 90 |
| 100 | 9 | 40 | 38 | −5 | −47 | −25 | 90 |
| 90 | 9 | 40 | 38 | −8 | −47 | −23 | 90 |
| 80 | 9 | 40 | 38 | −31 | −47 | 0 | 10 |
| 70 | 9 | 40 | 38 | −31 | −47 | 0 | 10 |
| 100 | 10 | 29 | 36 | −26 | −40 | 0 | 10 |
| 90 | 10 | 29 | 36 | −26 | −40 | 0 | 10 |
| 80 | 10 | 29 | 36 | −5 | −40 | −20 | 90 |
| 70 | 10 | 29 | 36 | −8 | −40 | −18 | 90 |
| 100 | 11 | 15 | 35 | 0 | −46 | −4 | 23 |
| 90 | 11 | 15 | 35 | 0 | −46 | −4 | 24 |
| 80 | 11 | 15 | 35 | −4 | −46 | 0 | 10 |
| 70 | 11 | 15 | 35 | −4 | −46 | 0 | 10 |
| 100 | 13 | 3 | 30 | 8 | −45 | 4 | 10 |
| 90 | 13 | 3 | 30 | 8 | −45 | 4 | 10 |
| 80 | 13 | 3 | 30 | 12 | −45 | 0 | 10 |
| 70 | 13 | 3 | 30 | 12 | −45 | 0 | 10 |
| 100 | 14 | 0 | 19 | 27 | −46 | 0 | 10 |

*(continued on next page)*

*(continued from previous page)*

| SOH (%) | Hour | SPV (kW) | WES (kW) | Grid (kW) | Load (kW) | BESS (kW) | SOC (%) |
|---|---|---|---|---|---|---|---|
| 90 | 14 | 0 | 19 | 27 | −46 | 0 | 10 |
| 80 | 14 | 0 | 19 | 27 | −46 | 0 | 10 |
| 70 | 14 | 0 | 19 | 27 | −46 | 0 | 10 |
| 100 | 15 | 0 | 12 | 33 | −45 | 0 | 10 |
| 90 | 15 | 0 | 12 | 33 | −45 | 0 | 10 |
| 80 | 15 | 0 | 12 | 33 | −45 | 0 | 10 |
| 70 | 15 | 0 | 12 | 33 | −45 | 0 | 10 |
| 100 | 16 | 0 | 8 | 38 | −47 | 0 | 10 |
| 90 | 16 | 0 | 8 | 38 | −47 | 0 | 10 |
| 80 | 16 | 0 | 8 | 38 | −47 | 0 | 10 |
| 70 | 16 | 0 | 8 | 38 | −47 | 0 | 10 |
| 100 | 17 | 0 | 6 | 41 | −47 | 0 | 10 |
| 90 | 17 | 0 | 6 | 41 | −47 | 0 | 10 |
| 80 | 17 | 0 | 6 | 41 | −47 | 0 | 10 |
| 70 | 17 | 0 | 6 | 41 | −47 | 0 | 10 |
| 100 | 18 | 0 | 5 | 27 | −31 | 0 | 10 |
| 90 | 18 | 0 | 5 | 27 | −31 | 0 | 10 |
| 80 | 18 | 0 | 5 | 27 | −31 | 0 | 10 |
| 70 | 18 | 0 | 5 | 27 | −31 | 0 | 10 |
| 100 | 19 | 0 | 5 | 40 | −45 | 0 | 10 |
| 90 | 19 | 0 | 5 | 40 | −45 | 0 | 10 |
| 80 | 19 | 0 | 5 | 40 | −45 | 0 | 10 |
| 70 | 19 | 0 | 5 | 40 | −45 | 0 | 10 |
| 100 | 20 | 0 | 7 | 28 | −36 | 0 | 10 |
| 90 | 20 | 0 | 7 | 28 | −36 | 0 | 10 |
| 80 | 20 | 0 | 7 | 28 | −36 | 0 | 10 |
| 70 | 20 | 0 | 7 | 28 | −36 | 0 | 10 |
| 100 | 21 | 0 | 10 | 33 | −43 | 0 | 10 |
| 90 | 21 | 0 | 10 | 33 | −43 | 0 | 10 |
| 80 | 21 | 0 | 10 | 33 | −43 | 0 | 10 |
| 70 | 21 | 0 | 10 | 33 | −43 | 0 | 10 |
| 100 | 22 | 0 | 12 | 21 | −33 | 0 | 10 |
| 90 | 22 | 0 | 12 | 21 | −33 | 0 | 10 |
| 80 | 22 | 0 | 12 | 21 | −33 | 0 | 10 |
| 70 | 22 | 0 | 12 | 21 | −33 | 0 | 10 |
| 100 | 23 | 0 | 13 | 32 | −45 | 0 | 10 |
| 90 | 23 | 0 | 13 | 32 | −45 | 0 | 10 |
| 80 | 23 | 0 | 13 | 32 | −45 | 0 | 10 |
| 70 | 23 | 0 | 13 | 32 | −45 | 0 | 10 |
| 100 | 24 | 0 | 12 | 33 | −45 | 0 | 10 |
| 90 | 24 | 0 | 12 | 33 | −45 | 0 | 10 |
| 80 | 24 | 0 | 12 | 33 | −45 | 0 | 10 |
| 70 | 24 | 0 | 12 | 33 | −45 | 0 | 10 |

## References


[1] Xiaoyuan Li, Zhe Tian, Xia Wu, Wei Feng, and Jide Niu. Optimal planning for hybrid renewable energy systems under limited information based on uncertainty quantification. *Renewable Energy*, 237:121866, 2024.

[2] Abdullahi Mohamed Samatar, Saad Mekhilef, Hazlie Mokhlis, Mostefa Kermadi, and Obaid Alshammari. Performance analysis of hybrid off-grid renewable energy systems for sustainable rural electrification. *Energy Conversion and Management: X*, 24:100780, 2024.

[3] Asmita Ajay Rathod and S. Balaji. Optimization of stand-alone hybrid renewable energy system based on techno-socio-enviro-financial perspective using improved red-tailed hawk algorithm. *Applied Energy*, 376:124137, 2024.

[4] Chukwuemeka Emmanuel Okafor and Komla Agbenyo Folly. Design and implementation of a control system for multifunctional applications of a battery energy storage system (BESS) in a power system network. *Cleaner Energy Systems*, 9:100153, 2024.

[5] Vitor Volpato Goulart, José Antonio Rodrigues Neto, and Ricardo Rüther. Method of techno-economic analysis of battery energy storage system (BESS) function-stacking for medium voltage connected consumers. *Journal of Energy Storage*, 83:110754, 2024.

[6] Dongxu Ouyang, Bo Liu, Jian Huang, and Zhirong Wang. Degradation and safety performance of lithium-ion cells under high-rate charging/discharging scenarios. *Process Safety and Environmental Protection*, 185:76–85, 2024.

[7] Santosh Chavan, Seo Eun Son, B. Venkateswarlu, Sang Woo Joo, and Sung Chul Kim. Impact of external heating and state of charge on discharge performance and thermal runaway risk in 21700 li-ion batteries. *Case Studies in Thermal Engineering*, 63:105299, 2024.

[8] Laiquan Lv, Shengyao Huang, Yang Zou, Xinyi Wang, and Hao Zhou. Thermal performance investigation of a medium-temperature pilot-scale latent heat thermal energy storage system: The constant and step temperatures charging and discharging. *Renewable Energy*, 225:120195, 2024.

[9] Qi Wang, Yandong Gu, Tao Zhu, Lantian Ge, and Yibo Huang. SOH estimation of lithium batteries based on ICA and WOA-RBF algorithm. *Energy Engineering*, 121(11):3221–3239, 2024.

[10] Minggang Zheng and Xing Luo. Joint estimation of state of charge (SOC) and state of health (SOH) for lithium ion batteries using support vector machine (SVM), convolutional neural network (CNN) and long sort term memory network (LSTM) models. *International Journal of Electrochemical Science*, 19(9):100747, 2024.

[11] R. Shyni and M. Kowsalya. An LSTM-DDPG framework power management strategy for a heterogeneous energy storage system in a standalone DC microgrid. *Journal of Energy Storage*, 104:114437, 2024.

[12] W. Merrouche, M. Trari, L. Djellal, M. Mammeri, H. Tebibel, S. Blaifi, Lee Wai Chong, S. Ould-amrouche, and B. Boussaha. Improved model and simulation tool for dynamic SOH estimation and life prediction of batteries used in PV systems. *Simulation Modelling Practice and Theory*, 119:102590, 2022.

[13] M. H. Elkholy, Tomonobu Senjyu, Mahmoud Elymany, Mahmoud M. Gamil, M. Talaat, Hasan Masrur, Soichiro Ueda, and Mohammed Elsayed Lotfy. Optimal resilient operation and sustainable power management within an autonomous residential microgrid using african vultures optimization algorithm. *Renewable Energy*, 224:120247, 2024.

[14] G. Suresh, D. Prasad, and M. Gopila. An efficient approach based power flow management in smart grid system with hybrid renewable energy sources. *Renewable Energy Focus*, 39:110–122, 2021.

[15] Xiaofen Fang, Zijie Chen, and JianQing Li. Optimized multi-head self-attention mechanism for SOH prediction in lithium-ion battery energy storage systems within microgrids. *Electric Power Systems Research*, 238:111182, 2025.

[16] Adani Solar. Adani solar 72-cell 300–330 Wp module datasheet. https://loopsolar.com/datasheet/adani-solar/datasheet-adani-solar-72-cell-300-330-Wp-India.pdf. Accessed: 8 Dec. 2024.

[17] PVlib. pvlib.iotools.get_pvgis_tmy function documentation. https://pvlib-python.readthedocs.io/en/v0.11.1/reference/generated/pvlib.iotools.get_pvgis_tmy.html. Accessed: 8 Dec. 2024.

[18] European Commission. Photovoltaic geographical information system (PVGIS). https://joint-research-centre.ec.europa.eu/photovoltaic-geographical-information-system-pvgis_en. Accessed: 8 Dec. 2024.

[19] Nationwide Energy. Endurance 50 kW turbine (25m tower) datasheet. http://www.nationwideenergy.co.uk/downloads/Endurance%2050kw%20turbine%20(25m%20tower).pdf. Accessed: 8 Dec. 2024.

[20] NASA. POWER project. https://power.larc.nasa.gov/. Accessed: 8 Dec. 2024.

[21] Vijay Mohan Nagulapati, Hyunjun Lee, DaWoon Jung, Boris Brigljevic, Yunseok Choi, and Hankwon Lim. Capacity estimation of batteries: Influence of training dataset size and diversity on data driven prognostic models. *Reliability Engineering & System Safety*, 216:108048, 2021.